EURASIP Journal on Applied Signal Processing 2004:9, 1321–1329

Gaussian Channel Model for Mobile Multipath Environment

D. D. N. Bevan
Harlow Laboratories, Nortel Networks, Harlow, Essex CM17 9NA, UK
Email: ddnb@nortelnetworks.com

V. T. Ermolayev
Communication Systems Research Department, MERA Networks, Nizhny Novgorod 603126, Russia
Email: ermol@mera.ru

A. G. Flaksman
Communication Systems Research Department, MERA Networks, Nizhny Novgorod 603126, Russia
Email: flak@mera.ru

I. M. Averin
Communication Systems Research Department, MERA Networks, Nizhny Novgorod 603126, Russia
Email: ave@mera.ru

Received 28 May 2003; Revised 5 February 2004

A model of an angle-spread source is described, termed the "Gaussian channel model" (GCM). This model is used to represent signals transmitted between a user equipment and a cellular base station. It assumes a Gaussian law of the scatterer occurrence probability, depending upon the scatterer distance from the user. The probability density function of the angle of arrival (AoA) of the multipath components is derived for an arbitrary angle spread. The "wandering" of the "centre of gravity" of the scattering source realisation is investigated, which is in turn due to the nonergodicity of the angle-scatter process. Numerical results obtained with the help of the sum-difference bearing method show the dependence of the AoA estimation accuracy on the spread-source model.

Keywords and phrases: scattering, angle spread, channel model, angle-of-arrival estimation, multibeam.

1. INTRODUCTION

The implementation of smart antennas at macrocellular base stations (BSs) is expected significantly to enhance the capacity of wireless networks [1, 2]. Various algorithms for adaptive array signal processing have been proposed and investigated [2, 3, 4]. The effectiveness of these algorithms depends on the behaviour of the fading channel and in particular on the degree of azimuthal dispersion in the channel. Therefore, accurate statistical channel models are required for the testing of these adaptive algorithms. These models must be realistic and close to real-life channels in order to replicate the angle of arrival (AoA) distribution of the multipath components.

The propagation channel between the BS and the user equipment (UE) is generally held to be reciprocal in most respects. However, the azimuthal angle dispersions seen at the BS and UE antenna differ significantly from each other. The classical Clarke channel model [5] assumes a uniform probability density function (pdf) of the incoming rays at the UE antenna. However, if the BS antenna array is elevated above the surrounding scatterers, then the rays incoming to the BS are concentrated in some smaller range of azimuth angles than those incoming to the UE. Note also that Clarke's model provides the well-known "rabbit-ear" characteristic of the classical Doppler spectrum of signals seen both at the BS and at the UE. Some statistical propagation models which include the azimuthal dispersion at the BS have been developed in [6, 7, 8]. For example, the channel model proposed in [7] is based on a geometrical construction, and assumes that scatterers are uniformly distributed within the area of a circle centred at the UE antenna. This means that the AoA of the multipath components at the BS will be restricted to an angular region dependent both upon the circle

radius and upon the distance between BS and user. However, in a real-life channel, the scatterer distribution around the UE can differ significantly from uniform. Therefore, other researchers [9, 10, 11] have proposed other more realistic models based on a Gaussian distribution of scatterer location.

The goal of this paper is to analyse further the Gaussian proposal for the scatterer distribution. We assume that the scatterers can be situated in *any* point in the horizontal plane. In this model, the probability of occurrence of the scatterer location decreases in accordance with a Gaussian law when its distance from the UE antenna increases. Therefore, we call this model the "Gaussian channel model (GCM)." We believe that such an assumption about the scatterer location is closer to the real-life environment than some of the other models mentioned above. Therefore, as we will demonstrate later, the comparison of the obtained pdf of AoA of the multipath for the GCM with the measured results presented in [8] gives very good agreement. Note also that, like Clarke's model, the proposed GCM also provides the classical Doppler signal spectrum.

It is a likely supplementary requirement for future cellular communication systems that they will be capable of determining the user position within a cell site. One way of doing this is via "triangulation," whereby the angular bearing of the user is estimated at multiple cellsites (this process is also known as "direction finding"). UE position is estimated as the point where these bearing lines intersect. Thus, in order to carry out triangulation, an estimate of the AoA of the UE signal is required. We consider the "sum-difference bearing method" (SDBM) algorithm for AoA estimation. It was selected from a number of techniques that had been investigated (see, e.g., [12, 13, 14]). The SDBM algorithm is similar to the principle used in monopulse tracking radars, wherein a hybrid junction is used to extract the sum and difference of a received pulse [12]. Note that the tracking radar is able to serve just one user. However, the multibeam antenna arrays at the BS can serve all the users located in the given cell. More details of this SDBM algorithm will be provided later.

One of the major aims of the BS is to achieve a high capacity. To maximise the downlink capacity, it has been proposed elsewhere to use multibeam or beamformed antenna arrays to cover each sector of the cell handled by the BS [15]. Such an antenna array could also be applied to estimate the AoA. Therefore, in this paper, the dependence of the AoA estimation accuracy on the spread source model is also considered for the BS using a multibeam antenna. In this configuration, the beamformer creates three fixed beams per 120°-azimuth sector, generated from a facet containing 6-off $\lambda/2$-spaced columns of dual-polar antenna elements. These beams improve the coverage and capacity of the macrocell, and are expected to have greatest application within the urban macrocellular environment, where the need for maximum capacity is the greatest. Simulation results are presented for the case of a Rayleigh fading channel and for this antenna configuration.

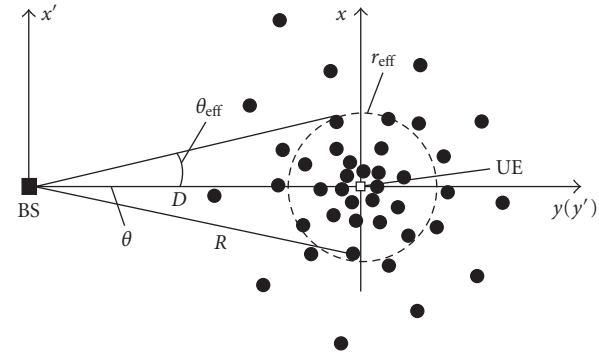

Figure 1: Illustration of the Gaussian channel model.

2. GAUSSIAN CHANNEL MODEL AND THE PDF OF THE AOAS OF MULTIPATH COMPONENTS SEEN AT THE BASE STATION

The signal received by the BS is a sum of many signals reflected from different scatterers randomly situated around the UE antenna. The AoAs of the multipath signal components are thus various and random. Therefore, the set of the scatterers can be considered collectively as a spread source, and the angle spread is a measure used to determine the angular dispersion of the channel.

Here we present the details of the GCM and derive an analytical expression for the pdf of the AoAs of multipath components as observed at the BS.

First of all, we list the initial assumptions used for creating the channel model. We assume that

(i) the scattered signals arrive at BS in the horizontal plane, that is, the proposed GCM is two dimensional and the elevation angle is not taken into account;

(ii) each scatterer is an omnidirectional reradiating element and the plane wave is reflected directly to the BS without influence from other scatterers (i.e., we have only "single-bounce" scattering paths);

(iii) the direct path from the UE to BS antenna is infinitely attenuated;

(iv) the reflection coefficient from each scatterer has unity amplitude and random phase;

(v) the probability of the (random) scatterer location is independent of azimuth angle (from the UE), and decreases if its distance from the UE antenna increases. This dependence has a Gaussian form.

The last of these assumptions distinguishes our channel model from many of the other known models [5, 6, 7].

Thus we can write that

$$p(r,\varphi) = \frac{1}{\pi r_{\text{eff}}^2} \exp\left(-\frac{r^2}{r_{\text{eff}}^2}\right), \tag{1}$$

where (r,φ) is the polar coordinate system centred at the UE, r is the distance to a given scatterer from the UE antenna, and r_{eff} is the radius at which the pdf decreases by a factor of e, that is, $p(r_{\text{eff}},\varphi) = e^{-1}p(0,\varphi)$. Figure 1 illustrates the GCM,

where D is the distance between the BS and UE antennas, and (x, y) are the rectangular coordinates.

In [7], a uniform scatterer distribution within the circle of radius r_0 around the UE was assumed. So for the model of [7], this means that the AoAs of multipath components seen at the BS are limited to the angular region $[-\theta_{\max} \cdots \theta_{\max}]$, where $\theta_{\max} = \sin^{-1}(r_0/D)$. However, for our GCM model, the AoAs of scattered signals as received at the BS are *not* restricted to any constrained angular region.

In order to derive the ensemble pdf of the AoA for the GCM (i.e., averaged over many model realisations), we choose the origin of the system coordinates (x', y') to be the location of the BS. This means that $x' = x$ and $y' = y + D$. We then transform to the polar coordinates (R, θ), where $x' = R\sin\theta$, $y' = R\cos\theta$, and the angle θ is measured relative to the line joining the BS and UE antennas. It is straightforward to show that the Jacobian of this transformation is equal to R. Furthermore, we have

$$r^2 = x^2 + y^2 = x'^2 + (y' - D)^2 = R^2 - 2RD\cos\theta + D^2. \quad (2)$$

As a result of substituting (2) into (1), we obtain that

$$p(R,\theta) = \frac{R}{\pi r_{\text{eff}}^2} \cdot \exp\left(-\frac{D^2}{r_{\text{eff}}^2}\right) \cdot \exp\left(-\frac{R^2 - 2RD\cos\theta}{r_{\text{eff}}^2}\right). \quad (3)$$

In order to derive the one-dimensional pdf of the AoA (i.e., the power angle density) of the multipath components as seen at the BS, an integration over the radius R must be carried out. Therefore, the pdf is expressed as the following integral:

$$p(\theta) = \int_0^\infty p(R,\theta)\,dR = \frac{1}{\pi r_{\text{eff}}^2} \cdot \exp\left(-\frac{D^2}{r_{\text{eff}}^2}\right) \int_0^\infty \exp\left(-\frac{R^2 - 2RD\cos\theta}{r_{\text{eff}}^2}\right) R\,dR. \quad (4)$$

This integral can be calculated analytically and a closed-form solution is obtained. To do this, take into account that (see [16, equation 3.462.1])

$$\int_0^\infty x^{\nu-1} \exp(-\beta x^2 - \gamma x)\,dx = (2\beta)^{-\nu/2}\Gamma(\nu)\exp\left(\frac{\gamma^2}{8\beta}\right) C_{-\nu}\left(\frac{\gamma}{\sqrt{2\beta}}\right), \quad (5)$$

where $\text{Re}(\nu, \beta) > 0$, $\Gamma(\nu)$ is the gamma function, and $C_p(z)$ is the function of the parabolic cylinder. In our case, we have $\nu = 2$, $\beta = r_{\text{eff}}^{-2}$, and $\gamma = -2Dr_{\text{eff}}^{-2}\cos\theta$. If $\nu = 2$, then the function $C_{-2}(z)$ can be expressed in terms of the probability integral $\Phi(z)$ (see [16, equation 9.254.2][1]), that is,

$$C_{-2}(z) = -\exp\left(\frac{z^2}{4}\right)\sqrt{\frac{\pi}{2}}\left\{z\left[1 - \Phi\left(\frac{z}{\sqrt{2}}\right)\right] - \sqrt{\frac{2}{\pi}}\exp\left(-\frac{z^2}{2}\right)\right\}, \quad (6)$$

where the probability integral $\Phi(x) = (2/\sqrt{\pi})\int_0^x \exp(-t^2)dt$.

Take into account that $z = -\sqrt{2}Dr_{\text{eff}}^{-1}\cos\theta$, $\Gamma(2) = 1$, and $\Phi(z)$ is an odd function of its argument z. As a result of straightforward transformations, we can obtain from (5) and (6) that the desired one-dimensional pdf $p(\theta)$ of AoA of the multipath components is given by

$$p(\theta) = \frac{1}{2\pi} \cdot \exp\left(-\frac{D^2}{r_{\text{eff}}^2}\right) \times\left\{1 + \sqrt{\pi}\frac{D}{r_{\text{eff}}}\cos\theta \cdot \exp\left(\frac{D^2}{r_{\text{eff}}^2}\cos^2\theta\right) \cdot \left[1 + \Phi\left(\frac{D}{r_{\text{eff}}}\cos\theta\right)\right]\right\}. \quad (7)$$

It is convenient to introduce the angle $\theta_{\text{eff}} = \sin^{-1}(r_{\text{eff}}/D)$. Then (7) can be rewritten as

$$p(\theta) = \frac{1}{2\pi} \cdot \exp\left(-\frac{1}{\sin^2\theta_{\text{eff}}}\right) \times\left\{1 + \sqrt{\pi}\frac{\cos\theta}{\sin\theta_{\text{eff}}} \cdot \exp\left(\frac{\cos^2\theta}{\sin^2\theta_{\text{eff}}}\right) \cdot \left[1 + \Phi\left(\frac{\cos\theta}{\sin\theta_{\text{eff}}}\right)\right]\right\}. \quad (8)$$

Thus the pdf $p(\theta)$ depends only upon $\cos\theta$. The effective angle spread for this pdf can be introduced as $\Delta = 2\theta_{\text{eff}}$. The pdf $p(\theta)$ is an even function of its argument θ.

The expression (8) is true in the general case. However, this formula takes a very simple form for the case of small angle spread $\theta_{\text{eff}} \ll \pi$ when $\sin\theta \approx \theta$. In this case, the pdf is approximately given by

$$p(\theta) \approx \frac{1}{\sqrt{\pi\theta_{\text{eff}}^2}} \cdot \exp\left(-\frac{\theta^2}{\theta_{\text{eff}}^2}\right) \quad (9)$$

and described by a (one-dimensional) Gaussian pdf with zero mean and variance $\sigma^2 = 0.5\theta_{\text{eff}}^2$.

Figure 2 shows the pdf $p(\theta)$ of the AoA of the multipath components for the different values $\theta_{\text{eff}} = 10°, 30°$, and $50°$. The solid and dashed curves correspond to the exact formula (8) and to its Gaussian approximation (9), respectively. We can see that the exact and Gaussian PDFs are very close to each other for a large interval of θ_{eff} up to $\theta_{\text{eff}} \le 0.5$ (or $\theta_{\text{eff}} \le 30°$). Actually, it is quite simple and intuitive to see how the complex pdf of the exact formula (8) should

[1] N.B. There is a minor typographical error (a missing factor of -1) in the version of this equation printed in [16], which is corrected within the addenda of the original Russian version.

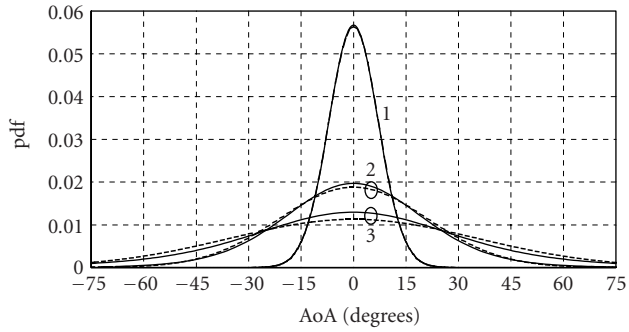

FIGURE 2: The pdf of the AoA of the multipaths at the BS. The angle spread is equal to 20, 60, and 100 degrees (curves 1, 2, 3, respectively). The solid and dashed curves correspond to the exact formula (8) and its Gaussian approximation (9), respectively.

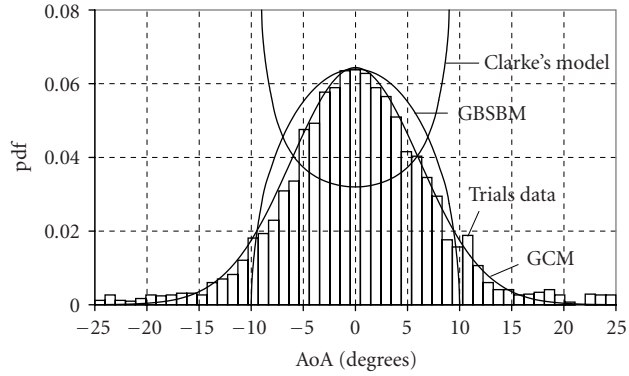

FIGURE 3: The PDFs for the AoA of the multipath components at the BS for GCM, GBSBM, Clarke's models, and for the measured histograms.

equal a one-dimensional pdf for small angle spreads. At these small angles, the lines bounding different small "slices" of the two-dimensional pdf are nearly parallel, and so it is as if we are calculating the marginal pdf of the two-dimensional spatial pdf along the x-axis. Since the marginal pdf of a two-dimensional Gaussian distribution is a one-dimensional Gaussian distribution, our approximate result (9) is intuitively of the correct form.

The comparison of the theoretical pdf against real measurement data is of course of interest in order both to validate and to parameterise the GCM. Histograms of the estimated azimuthal power angle density and scatterer occurrence probabilities are presented by the authors of [8]. This measurement data was obtained in Aarhus with a BS antenna located 12 m above the rooftop level. We wish to take this measured data and compare it to the three proposed theoretical channel models: (1) our GCM of (8), (2) the geometrical-based single-bounce model (GBSBM) developed in [7] (in which the scatterers are assumed to be uniformly randomly distributed within the area of a circle), and (3) Clarke's model [5, 17] (in which the scatterers are assumed to lie on the circumference of a circle).

It was derived in [7] that the pdf of the AOA of the multipath components for GBSBM is given by

$$p(\theta) = \begin{cases} \dfrac{2\cos(\theta)\sqrt{\sin^2\theta_{\max} - \sin^2\theta}}{\pi \sin^2\theta_{\max}}, & -\theta_{\max} \le \theta \le \theta_{\max}, \\ 0, & \text{otherwise}, \end{cases} \tag{10}$$

where $\theta_{\max} = \sin^{-1}(r_0/D)$ and r_0 is the radius of the circle within which all the scatterers are uniformly distributed.

Whilst we omit the derivation here, for reasons of brevity, it can be shown that the pdf of the AOA of the multipath components for Clarke's model is equal to

$$p(\theta) = \frac{1}{\pi}\frac{1}{\cos^2\theta}\frac{1}{\sqrt{\tan^2\theta_{\max} - \tan^2\theta}}, \tag{11}$$

where in this case, when calculating $\theta_{\max}$, r_0 has the meaning of the radius of the circle periphery on which the scatterers are uniformly distributed.

Figure 3 shows the PDFs for the AoA of the multipath components at the BS for GCM, GBSBM, Clarke's models, and the measured scatterer occurrence probability histograms taken from [8]. We have chosen the model parameters $(\theta_{\max}, \theta_{\text{eff}})$ so that the best agreement was obtained for each model. For both the GBSBM and Clarke's models, the value chosen was $\theta_{\max} = 10°$, and for GCM, $\theta_{\text{eff}} = 8.8°$. It can be seen that the GCM ensures the best agreement with real-life results for the whole angular region and especially for the tails of histogram. Clarke's model produces the worst match to the real-life data.

The measured data and experimental models described above discuss the "ensemble" statistics of the spread source. By ensemble statistics, we mean that these statistics are averaged over a large number of individual measurements or individual model realisations. However, in practice, we would deal with single cases (i.e., in "real-life") or single-model realisations (i.e., during simulation). It seems reasonable to postulate that the angle-spread behaviour of the source will be nonergodic. That is to say, the statistics of any given realisation (averaged over time) will, in general, be different from the *ensemble* statistics (averaged over *all* realisations and *all* time). So in practice, in any single realisation of the angle-spread model, we will see a limited number of *discrete* scattering centres creating a "lumpy" AoA distribution function, rather than an infinite number of scatterers creating a continuous "smooth" distribution, as observed from the ensemble statistics. If this limited number of discrete scattering centres is particularly small, then their "centre of gravity (CofG)" may "wander" about the true bearing of the UE. The CofG, to be defined in more detail below, is simply a power-weighted average AoA. As an example, in one realisation of the scattering model, *all* of the scattering centres may, purely by chance, be located on the left-hand side of the true UE bearing, which would bias the *apparent* (i.e., estimated) bearing of the UE to the left. Conversely, in another realisation, all of the scattering centres may, again by chance, be located on the right-hand side of the true UE bearing, which would bias the apparent bearing of the UE to the right. So this

apparent change of the UE bearing for different realisations of the scattering model, which we term the "wandering" of the "CofG" is a direct consequence of the nonergodicity of the angle-scattering model. This wandering is more marked when the mean number of scattering sources is low, because if we have a large number of scattering sources, then it would be *extremely* unlikely for *all* of them to be lying on the same side of the UE (assuming that all scatterer locations are independent). In fact, we will show later that this "wandering of the CofG" phenomenon is a significant contributor to the overall estimation error of the UE bearing.

For reasons described above, the variance of the wandering of the CofG depends on the number of scatterers situated around the UE antenna. Let N be the number of scatterers and $\theta_1, \theta_2, \ldots, \theta_N$ some random values of AoAs of the signal from these scatterers. Assume, for simplicity, that all of the sources have equal power. Then the CofG of the received signal for this particular realisation is equal to

$$\widetilde{\theta} = \frac{1}{N}(\theta_1 + \theta_2 + \cdots + \theta_N). \tag{12}$$

The expectation of the random value $\widetilde{\theta}$ is equal to zero (i.e., $\langle\widetilde{\theta}\rangle = 0$) and its variance can be obtained from the integral

$$\sigma^2_{N\theta} = \iint \cdots \int \frac{1}{N^2}(\theta_1 + \theta_2 + \cdots + \theta_N)^2 \times p(\theta_1, \theta_2, \ldots, \theta_N)\, d\theta_1 d\theta_2 \cdots d\theta_N, \tag{13}$$

where $p(\theta_1, \theta_2, \ldots, \theta_N)$ is the joint pdf of the AoAs $\theta_1, \theta_2, \ldots, \theta_N$. Since these AoAs are assumed to be independent random values, the joint pdf can be presented as the product of individual PDFs, that is, $p(\theta_1, \theta_2, \ldots, \theta_N) = p(\theta_1)p(\theta_2)\cdots p(\theta_N)$, where the function $p(\theta_i)$ $(i = 1, 2, \ldots, N)$ is given by formula (8).

The *expected* azimuth angle of each angle-spread source is equal to zero due to the symmetry of the pdf (8) of the multipath component AoAs, that is, $\langle\theta_i\rangle = 0$. Thus the N-dimensional integral (13) can be rewritten as the sum of N identical one-dimensional integrals, that is,

$$\sigma^2_{N\theta} = \frac{1}{N^2}\sum_{i=1}^{N}\int \theta_i^2 p(\theta_i)\, d\theta_i = \frac{\sigma^2_{1\theta}}{N}, \tag{14}$$

where $\sigma^2_{1\theta}$ is the variance of the AoA of a single scatterer, equal to

$$\sigma^2_{1\theta} = \int \theta^2 p(\theta) d\theta \tag{15}$$

and pdf $p(\theta)$ is defined by formula (8).

So (14) and (15) give the mean squared value for the wandering of the CofG of the spread source when we assume N scatterers of the same amplitude.

For small $\theta_{\text{eff}} \ll 1$, the pdf $p(\theta)$ has Gaussian form (9). Substituting (9) into (15) and carrying out the integration in (15), we obtain that $\sigma_{1\theta} = \theta_{\text{eff}}/\sqrt{2}$. Hence it can be found from (14) that the wandering of the CofG is equal to

$$\sigma_{N\theta} = \frac{\theta_{\text{eff}}}{\sqrt{2N}}. \tag{16}$$

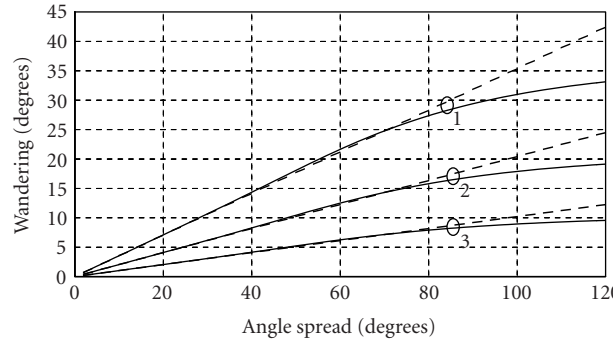

Figure 4: The source C of G wandering versus angle spread Δ for the different numbers of scatterers $N = 1, 3, 12$ (curves 1, 2, 3, respectively). The solid and dashed curves correspond to the exact formula (8) and its Gaussian approximation (9), respectively.

Figure 4 shows the wandering $\sigma_{N\theta}$ of the CofG of the source versus angle spread Δ for different numbers of scatterers $N = 1, 3, 12$ (curves 1, 2, 3). The solid and dashed curves correspond to the exact formula (8) and its Gaussian approximation (9), respectively. We can see that the exact and Gaussian PDFs are very close to each other for a large interval of θ_{eff} up to $\approx 40^\circ$.

The CofG of the scattering sources gives the best unbiased estimate of the true UE bearing, albeit that it is an estimate with high variance (i.e., high mean squared error) when the number of scattering centres is small. So the aim of our AoA estimation processing is to estimate this CofG from a limited-time snapshot of noisy received signal. The receiver noise will add an additional error term to the final bearing estimation error. However, it can be seen from the foregoing analysis that even using "perfect" CofG estimation algorithms on long samples of high signal-to-noise-ratio (SNR) received signal, there will still be a residual irreducible error if the number of scattering centres is small. This is because of the wandering of the CofG, which in turn is due to the nonergodicity of the spread source.

3. AOA ESTIMATION INCORPORATING THE GCM

We have stated above that the best estimate of the true UE bearing is given by estimating the CofG of the received signal (i.e., for a given single realisation of the scattering). However, even using a "perfect" AoA estimation algorithm, we would suffer from irreducible errors due to the "wandering" of the scatterer CofG. For reasons of implementation simplicity, we may well in practice contemplate using a less-than-perfect AoA estimation algorithm if (a) the implementation of this less-than-perfect algorithm is simple, and hence cheap to implement, and (b) the *additional* errors introduced by

the less-than-perfect algorithm (compared to an optimal algorithm) are small compared to the irreducible CofG wandering error which we must allow for in any case. So in this section, we consider just such a simplified AoA estimation process, which we term SDBM. This method was selected from a number of similar techniques which had been investigated because it was found to give the overall most accurate and most robust performance. The mathematical details of the SDBM technique will be presented later. However, the essence of the technique is to measure, average, and compare received signal powers (or amplitudes) received at the BS, as measured in adjacent beams. We assume, for the use of SDBM, that the BS already employs a multibeam antenna (typically with three deep-cusp beams) in each 120°-azimuth sector. The scattered signal from the user is received by each of the beams of the antenna, and the two adjacent beams receiving the highest signal powers are selected. For these beams, a set of functions, which we term "bearing curves," must be precalculated and stored. The exact form of these bearing curves depends upon the multibeam antenna patterns and upon the expected ensemble angle-spread distribution (which we argued earlier tends to Gaussian form at small angle spreads).

First of all, we determine the dependence of the average received power G at an arbitrary beam output on the angle location of the source with an angle spread Δ. Let $F(\theta)$ be the reception gain pattern of this beam and θ_0 be the centre of the spread source (i.e., the "true" UE bearing). Then the function $G(\theta_0)$ can be presented in form of a mathematical convolution of (i) a function representing the power beam pattern $|F(\theta_0)|^2$ of this beam as a function of the azimuth angle (θ) and (ii) a function $p(\theta)$ representing the (ensemble) pdf of the AoAs of signals received by the BS due to reflections from scatterers as a function of azimuth angle (θ), that is,

$$G(\theta_0) = \int_0^{\pi} |F(\theta)|^2 p(\theta - \theta_0)\, d\theta. \tag{17}$$

We can refer to the function (17) as a "beam pattern for a spread source," that is, what we call a "spread" beam pattern. If the spread of signals is a negligibly small quantity ($\theta_{\text{eff}} \to 0$), then we have a point source, and the pdf $p(\theta)$ in (8) tends to a delta function (i.e., $p(\theta) \to \delta(\theta - \theta_0)$). In this case, the function $G(\theta_0)$ is given by $G(\theta_0) = |F(\theta_0)|^2$, that is, it is simply equal to the power gain pattern of the beam, or to what we will term the "point source" beam pattern.

Now we provide the mathematical definition of what we have termed earlier the "bearing curves." If L is the number of the beams generated by the multibeam antenna, then we have a set of beam patterns $G_i(\theta)$ ($i = 1, 2, \ldots, L$) and each beam pattern is oriented in a given direction. The bearing curves $b_{i+1,i}$ ($i = 1, 2, \ldots, L-1$) for each adjacent beam pair ($i+1, i$) may be represented by a function $b_{i+1,i}(\theta)$ of the azimuth angle θ of the antenna according to the following equation:

$$b_{i+1,i}(\theta) = \frac{\sqrt{G_i(\theta)} - \sqrt{G_{i+1}(\theta)}}{\sqrt{G_i(\theta)} + \sqrt{G_{i+1}(\theta)}}. \tag{18}$$

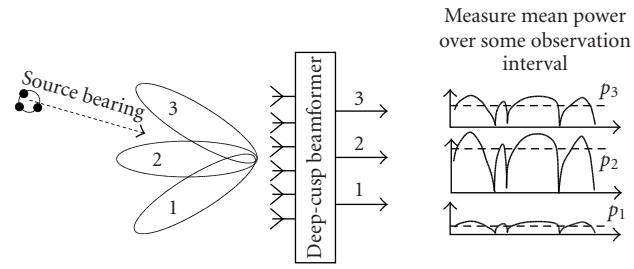

Figure 5: Applying the SDBM algorithm.

These bearing curves are precalculated and stored by the network. The precalculation takes place based on equation (17), and hence takes into account both the known multibeam patterns and the *expected* angle-spread distribution of the scattering channel (which we model as Gaussian with a given θ_{eff}). There is more discussion later about how we determine the expected angle spread.

To estimate the bearing of any given source, the received power from each beam of the antenna is measured over a predetermined observation interval by averaging over a large number of samples. The observation interval should be chosen to be long enough so that the effects of Doppler signal fading do not significantly impact the measured power.

The application of SDBM algorithm is shown in Figure 5. Let $p_i = |s_i(t) + n_i(t)|^2$ be the mean power measured at the output of the ith ($i = 1, 2, \ldots, L$) antenna beam, where $s_i(t)$ and $n_i(t)$ are the useful signal and additive white Gaussian noise (AWGN), respectively. The AWGN variance σ_0^2 is assumed to be the same for all of the different antenna beams. The bearing curves, per (18), are produced without regard to AWGN. That is to say, they only take into account ratios of sums and differences of expected *signal* amplitudes (without including noise or interference contributions). Therefore, for a more accurate estimation of AoA based on measured noisy samples, we need to take into account an *expected* noise power contribution for the measured signal, the value of which we subtract from the *measured* power signal of each beam after the averaging. In practice, this means that we use an estimated output signal power equal to $\widetilde{p}_i = |p_i - \sigma_0^2|$. The estimates $\widetilde{p}_i$ for all $i = 1, 2, \ldots, L$ are compared with each other and the two adjacent beams receiving the highest signal powers are selected. If the jth and $(j+1)$th beams have the highest output powers, then the sum-difference ratio $\hat{b}_{j+1,j} = (\sqrt{\widetilde{p}_j} - \sqrt{\widetilde{p}_{j+1}})/(\sqrt{\widetilde{p}_j} + \sqrt{\widetilde{p}_{j+1}})$ is calculated and the AoA is estimated by looking up the bearing θ corresponding to this ratio from the corresponding bearing curve $b_{j+1,j}(\theta)$ of (18).

Now we present simulation results for the SDBM technique in order to estimate the accuracy which can be achieved. Any one of a number of possible multibeam antenna designs could have been assumed for this simulation, but for this work, we have used the "deep-cusp" multibeam antenna design of [15]. The deep-cusp beamformer creates three fixed beams per each 120°-azimuth sector, generated from a facet containing 6-off $\lambda/2$-spaced columns of

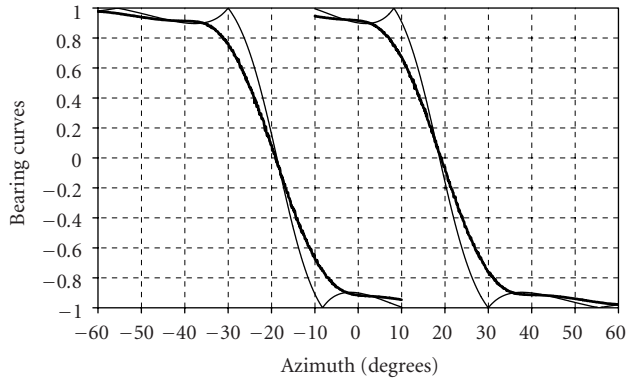

FIGURE 6: Bearing curves $b_{21}(\theta)$ (left-hand curves) and $b_{32}(\theta)$ (right-hand curves) for the point ($\Delta = 0°$) and spread ($\Delta = 17°$) sources (thin and thick curves, respectively).

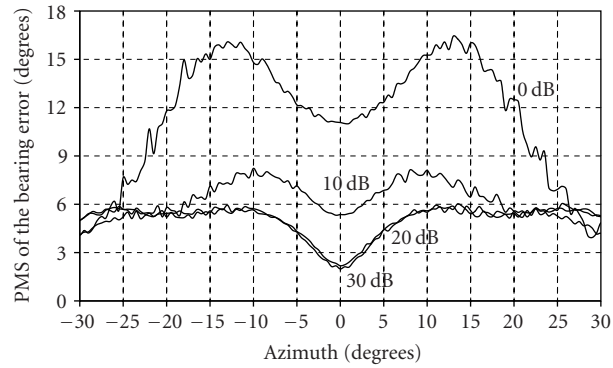

FIGURE 7: The rms of bearing estimation error for various SNRs and for the number of scatterers $N = 3$.

dual-polar antenna elements (although only a single polarisation is considered here). The angular spread of the source will be assumed to be equal to 17°, which corresponds to experimental results obtained in [8]. Two representative cases, for which the number of scatterers is specified as $N = 3$ and $N = 12$, will be simulated. There are two bearing curves $b_{21}(\theta)$ and $b_{32}(\theta)$ for the antenna configuration with three beams.

The bearing curves $b_{21}(\theta)$ and $b_{32}(\theta)$ for the point ($\Delta = 0°$) and spread ($\Delta = 17°$) sources are presented in Figure 6 (thin and thick curves, respectively). The left-hand curves are $b_{21}(\theta)$ and the right-hand curves are $b_{32}(\theta)$. It can be seen that these bearing curves have the steepest slope at the points where the beams cross. Estimation of the bearing of the point source is possible only in the angle intervals $[-30°, -10°]$ and $[10°, 30°]$. For the spread source, estimation of the bearing is possible over wider angle intervals $[-35°, 35°]$. It is assumed, of course, that to estimate the bearing of UEs for angles outside this range, we would construct additional bearing curves relating to the beam at the edge of this sector and its neighbour at the edge of the adjacent sector.

When estimating the AoA, the estimates $\widetilde{p}_1$, $\widetilde{p}_2$, and $\widetilde{p}_3$ of the mean signal power at the output of the ith ($i = 1, 2, 3$) antenna beam are compared with each other. If $\widetilde{p}_1 > \widetilde{p}_3$, then the ratio $\hat{b}_{21}$ is calculated and the AoA is estimated using the bearing curve $b_{21}(\theta)$. If $\widetilde{p}_1 < \widetilde{p}_3$, then the value $\hat{b}_{32}$ is calculated and the AoA is estimated according to the bearing curve $b_{32}(\theta)$.

Within the simulations, the samples of the complex signals were generated with a sampling period equal to 1 millisecond for three antenna beams. The maximum Doppler frequency f_d was set equal to 50 Hz. The observation interval was chosen to be 400 milliseconds, that is, approximately 50 times longer than the fading correlation interval. Various SNRs equal to 30, 20, 10 and 0 dB were simulated, where the SNR is defined by what the received SNR is for a point source located at the peak of the central beam. In order to average the results over all source directions, the true source angle θ_{true} was varied from $-40°$ to $+40°$ with a step size equal to 0.5°. A thousand experiments were carried out for each source direction, and different realisations of the (nonergodic) source model were applied for each of these experiments. For each source position, the root-mean-square (rms) Δ_θ of the bearing estimation error and the cumulative density function (CDF) of absolute value of AoA estimation error $|\hat{\theta}_j - \theta_{\text{true}}|$ were calculated.

The rms of the bearing estimation error is shown in Figure 7 for the number of scatterers $N = 3$ and for the given SNRs. We can see that, as expected, the rms of the bearing estimation error decreases when the SNR increases. For large SNRs (20 and 30 dB), the bearing estimation error lies within the range 2° to 6° (depending on the true source bearing) and is solely due to the random wandering of the CofG of the angle-spread source. For the lower SNRs, the bearing estimation error is larger, and depends also on AWGN power. The corresponding CDFs are presented in Figure 8. The CDFs in Figure 8 can be approximated by the CDF of a Gaussian function. Using this Gaussian approximation, we obtain that the standard deviation of the bearing estimation error is $\approx 4°$ for high SNRs and $N = 3$. As can be seen from Figure 4 (curves 2), this standard deviation is approximately equal to the standard deviation of the wandering of the CofG of the source with an angle spread $\Delta = 2\theta_{\text{eff}} = 17°$ ($\theta_{\text{eff}} = 8.5°$). Thus we can see that the bearing estimation error for high SNRs is conditioned by the nonergodicity of the source model. The highest bearing estimation errors are observed in the crossing area of the antenna beam patterns. This is because the beam gains are lower in this angular region, and so the effective received SNR is also lower in this region compared to what it would be for a source located close to the peak of the central beam. The CDF of the bearing estimation error for a larger number of scatterers $N = 12$ is also shown in Figure 8. Compared to the results for $N = 3$, the standard deviation of the bearing estimation error has decreased by a factor of approximately two for high SNRs, from $\approx 4°$ to $\approx 2°$. Like the results for $N = 3$, this also corresponds to Figure 4 and (14).

As is evident from the earlier discussion, the form of the bearing curves is different for different assumed channel angle spreads. This is because the first stage of the generation

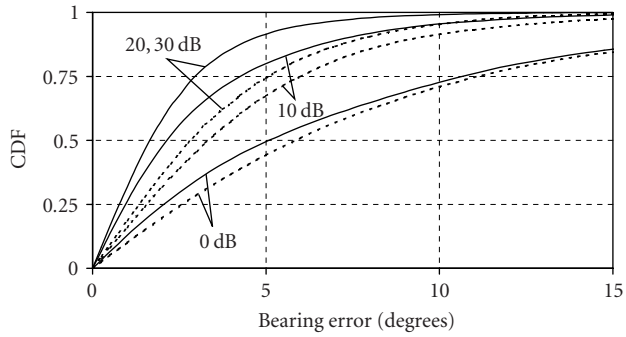

Figure 8: The CDFs of the bearing estimation error for various SNRs. The number of scatterers is $N = 12$ (solid curves) and $N = 3$ (dashed curves).

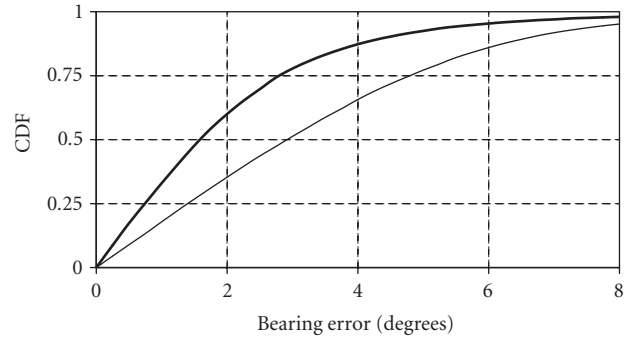

Figure 9: The CDF of the bearing estimation error using the "spread" bearing curve (thick curve) and "point source" bearing curve (thin curve) for SNR = 30 dB, angle spread $\Delta = 17^\circ$, and number of scatterers $N = 12$.

of the bearing curves involves a convolution of the *actual* beam pattern with the *assumed* angle-spread ensemble pdf. What if we didn't apply the preconvolution in the generation of the bearing curves, but simply used the bearing curve corresponding to "point source" beam patterns, even when the channel itself *does* exhibit angle spread? To answer this, it is interesting to examine the bearing errors when bearing curves generated for the point source are actually used for estimating AoA in a channel *with* angle spreading. Such comparative simulation results for the CDF of the bearing error are presented in Figure 9 for SNR = 30 dB and number of scatterers $N = 12$. The angle spread in the channel is equal to 17°. We can see that the bearing error has increased significantly due to the use of "nonmatched" bearing curves. In order to generate "matched" bearing curves, we need at least to have a reasonable estimate of the (ensemble) angle spread of the channel. In practice, this would be obtained through examination of published measured angle-spread data such as [8], and by matching the environment in which the multibeam BS is deployed (e.g., urban, suburban, rural) to the expected angle spread of the channel.

4. CONCLUSIONS

In this paper, we have developed a model for an angle-spread source which we term the Gaussian channel model (GCM). This model is suitable for representing the signal seen at the base station (BS) antenna, and assumes that the probability of the scatterer occurrence decreases in accordance with a Gaussian law when its distance from the user equipment (UE) antenna increases. Such an assumption about the scatterer location is closer to the real-life environment than some of the other known models. An analytical expression for the probability density function (pdf) of the multipath angle of arrival (AoA) at the BS has been derived for the general case of an arbitrary angle spread. It is shown that this pdf can be approximated by a Gaussian curve for sources with a small spread. The comparison of the obtained pdf of AoA of the multipath for the GCM with the published experimental results gives a better agreement than for some other known angle scattering models. However, in a real-life situation, we deal with a single realisation of the angle-spread source, that is, with a fixed finite number of *discrete* scattering centres. If this number is particularly small, then their center of gravity (CofG), defined as a power-weighted average AoA, may "wander" about the true bearing of the UE. The variance of this wandering of the CofG has been obtained. The dependence of the AoA estimation accuracy on the parameters of the spread source model has also been considered for a BS using a multibeam antenna, by carrying out simulations of the so-called sum-difference bearing method (SDBM) AoA estimation algorithm. It has been shown that for high SNRs, the bearing estimation errors are dominated by the wandering of the CofG of the spread source. This wandering is a consequence of the nonergodicity of the angle scattering process and is greater when the number of scattering sources is small.

REFERENCES

[1] J. C. Liberti and T. S. Rappaport, *Smart Antennas for Wireless Communications: IS-95 and Third Generation CDMA Applications*, Prentice Hall, Upper Saddle River, NJ, USA, 1999.

[2] J. B. Andersen, "Antenna arrays in mobile communications: gain, diversity, and channel capacity," *IEEE Antennas and Propagation Magazine*, vol. 42, no. 2, pp. 12–16, 2000.

[3] U. Vornefeld, C. Walke, and B. Walke, "SDMA techniques for wireless ATM," *IEEE Communications Magazine*, vol. 37, no. 11, pp. 52–57, 1999.

[4] R. A. Soni, R. M. Buehrer, and R. D. Benning, "Intelligent antenna system for cdma2000," *IEEE Signal Processing Magazine*, vol. 19, no. 4, pp. 54–67, 2002.

[5] R. H. Clarke, "A statistical theory of mobile-radio reception," *Bell System Technical Journal*, vol. 47, no. 6, pp. 957–1000, 1968.

[6] J. C. Liberti and T. S. Rappaport, "A geometrically based model for line-of-sight multipath radio channels," in *Proc. IEEE 46th Vehicular Technology Conference*, vol. 2, pp. 844–848, Atlanta, Ga, USA, April 1996.

[7] P. Petrus, J. H. Reed, and T. S. Rappaport, "Geometrical-based statistical macrocell channel model for mobile environments," *IEEE Trans. Communications*, vol. 50, no. 3, pp. 495–502, 2002.

[8] K. I. Pedersen, P. E. Mogensen, and B. H. Fleury, "A stochastic model of the temporal and azimuthal dispersion seen at

the base station in outdoor propagation environments," *IEEE Trans. Vehicular Technology*, vol. 49, no. 2, pp. 437–447, 2000.
[9] J. Fuhl, A. F. Molisch, and E. Bonek, "Unified channel model for mobile radio systems with smart antennas," *IEE Proceedings Radar, Sonar and Navigation*, vol. 145, no. 1, pp. 32–41, 1998.
[10] R. M. Buehrer, S. Arunachalam, K. H. Wu, and A. Tonello, "Spatial channel model and measurements for IMT-2000 systems," in *Proc. IEEE Vehicular Technology Conference*, vol. 1, pp. 342–346, Rhodes, Greece, May 2001.
[11] Lucent Technologies, "Proposal for a spatial channel model in 3GPP RAN1/RAN4," Contribution WG1#20(01)579 of Lucent Technologies to 3GPP-WG1, Busan, May 2001.
[12] M. I. Skolnik, Ed., *Radar Handbook*, McGraw-Hill, New York, NY, USA, 1970.
[13] O. Besson, F. Vincent, P. Stoica, and A. B. Gershman, "Approximate maximum likelihood estimators for array processing in multiplicative noise environments," *IEEE Trans. Signal Processing*, vol. 48, no. 9, pp. 2506–2518, 2000.
[14] S. Valaee, B. Champagne, and P. Kabal, "Parametric localization of distributed sources," *IEEE Trans. Signal Processing*, vol. 43, no. 9, pp. 2144–2153, 1995.
[15] M. S. Smith, M. Newton, and J. E. Dalley, "Multiple beam antenna," US Patent number 6,480,524, November 2002.
[16] I. S. Gradshteyn and I. M. Ryzhik, *Table of Integrals Series and Products*, Academic Press, New York, NY, USA, 1965.
[17] W. C. Jakes, Ed., *Microwave Mobile Communications*, John Wiley & Sons, New York, NY, USA, 1974.

D. D. N. Bevan received his M.Eng. in electronic and electrical engineering from Loughborough University of Technology in 1991. Since then, he has worked in the field of radio technology within the Wireless Technology Laboratories of Nortel Networks in Harlow, UK. His research interests include system modelling, array signal processing, and technologies for current and future wide-area and local-area wireless networking.

V. T. Ermolayev received his Ph.D. and the Doctor of Science degrees in radiophysics from Nizhny Novgorod State University in 1980 and 1996, respectively. He has worked with the Radiotechnical Institute, State University, and the scientific and technical company "Mera," Nizhny Novgorod, Russia. His research interests include array signal processing, space-time spectral analysis, signal parameter estimation and detection, and wireless communications.

A. G. Flaksman received his Ph.D. degree in radiophysics from Nizhny Novgorod State University in 1983. He has worked with the radiotechnical Institute, State University, and the scientific and technical company "Mera," Nizhny Novgorod, Russia. His research interests include array signal processing, space-time spectral analysis, signal parameter estimation and detection, and wireless communications.

I. M. Averin received his diploma (M.S.) in radiotechnics from Nizhny Novgorod Technical University in 2000. Since then, he has worked in the field of radio technology with the scientific and technical company "Mera," Nizhny Novgorod, Russia. He is also currently a postgraduate student in Nizhny Novgorod Technical University. His research interests include array signal processing, space-time spectral analysis, and wireless communications.